Journal of Molecular Biomarkers & Diagnosis

Desai, et al., J Mol Biomark Diagn 2015, 6:2
DOI: 10.4172/2155-9929.1000228

Research Article Open Access

A Novel Method for Mutation Analysis Using Genomic DNA Obtained from Immunohistochemistry-Stained Sections

Rupal Desai[1], Rajesh Patel[1], Lukas Amler[1], Hartmut Koeppen[2], Ian McCaffery[1], Gianni Luca[3], Astrid Kiermaier[1] and Rajiv Raja[1*]

[1]*Department of Oncology Biomarker Development, 1 DNA Way, Genentech Inc., South San Francisco, California, USA*

[2]*Department of Research Pathology, 1 DNA Way, Genentech Inc., South San Francisco, California, USA*

[3]*Departments of Oncologia Medica, Ospedale San Raffaele, Milan, Italy*

[*]**Corresponding author:** Rajiv Raja, Department of Oncology Biomarker Development, Genentech Inc., MS-461a, 640 East Grand Avenue, South San Francisco, CA 94080, USA, Tel: 650 225 3291; Fax: 650-467-7571; E-mail: raja.rajiv@gene.com

Rec date: Jan 27, 2015; **Acc date:** Mar 28, 2015; **Pub date:** Mar 30, 2015

Abstract

Background: Tumor biopsies obtained from patients are often limited in size and availability, and the ability to perform multiple diagnostic assays depends on the quantity and quality of the tissue. Here we describe and evaluate a method for performing DNA-based mutational analyses after immunohistochemistry analysis has been performed, using a single tissue section.

Method: Immunohistochemistry analysis was performed on 4-5 µm formalin-fixed paraffin-embedded tumor tissue sections and immunohistochemistry-stained sections were stored for subsequent genomic analysis. DNA was isolated from these immunohistochemistry-stained sections and DNA quality was assessed using a multiplex-polymerase chain reaction method as well as real time quantitative polymerase chain reaction of commonly used reference genes. Subsequently, genomic DNA was pre-amplified and mutations in *KRAS, BRAF, NRAS* and *PIK3CA* were detected by validated Taqman assays. Comparisons were made with results from unstained formalin-fixed paraffin-embedded sections obtained from the same paraffin block.

Results: Our results demonstrate that genomic DNA isolated from immunohistochemistry-stained and unstained formalin-fixed paraffin-embedded tissue sections are comparable in quality and are suitable for down-stream analysis using polymerase chain reaction based assays. We also found that the sensitivity and specificity in detecting hotspot mutations are comparable in both sources of genomic DNA. This study reports 100% concordance in detecting hotspot mutations in *KRAS, BRAF, NRAS* and *PIK3CA* using quantitative real-time polymerase chain reaction between stained and unstained formalin-fixed paraffin-embedded sections.

Conclusion: We conclude that by using our novel approach, it is possible to perform immunohistochemistry staining followed by genomic analysis using a single 4-5 µm section of formalin-fixed paraffin-embedded tissue.

Keywords: Biopsy; Formalin-fixed paraffin-embedded tissue; Immunohistochemistry; Genotyping; DNA analysis

Abbreviations

C_T: Cycle Threshold; FFPE: Formalin-Fixed Paraffin-Embedded; FISH: Fluorescent *in situ* Hybridization; gDNA: genomic DNA; H&E: Haematoxylin and Eosin; IHC: Immunohistochemical; IRB: Institutional Review Board; MND: Mutation Not Detected; PCR: Polymerase Chain Reaction; qRT-PCR: quantitative Real Time Polymerase Chain Reaction

Introduction

Histopathological and immunohistochemical (IHC) analysis have been the predominant methods used to diagnose cancer. A large number of genomic alterations such as gene amplifications, point mutations, translocations, deletions, or insertions have been extensively documented in various types of cancers [1,2].

However, only a small number of such alterations have been causally linked to cancer and they vary from tumor to tumor [3-5]. Identifying relationships between genomic alterations and cancer has provided a number of valuable targets for targeted therapies, such as *BRAF* mutations in melanoma [6,7] and *ALK* translocations in lung cancer [8,9]. Identifying genomic alterations along with histopathological and IHC analysis would enable clinicians to stratify patients based on the molecular characteristics of the tumor to deliver targeted therapies. Some well-known examples of such alterations and related therapies are vemurafenib for *BRAF*-mutant melanoma and crizotinib for lung cancers with EML4-ALK translocation.

The ability to perform multiple assays is often limited by the amount of patient sample available for biomarker assessments. Hence, being able to perform multiple assessments on a single section of tumor tissue would enable diagnostic testing in instances where the amount of tissue available is limited. Generally, clinical biopsies are preserved by fixing in formalin followed by embedding in paraffin for long-term storage. Formalin fixation greatly preserves the cellular architecture, which enables detailed histopathological and IHC analysis. Even though formalin-fixing is generally found to be deleterious for preserving the integrity of nucleic acids, DNA is relatively well-preserved in formalin-fixed paraffin-embedded (FFPE)

tissue compared to RNA. DNA from FFPE tissues have been reliably used for genomic analysis such as sequencing and polymerase chain reaction (PCR) in various tissue types [10-15]. Since FFPE specimens are easily obtainable from the tissue archives, they can serve as an excellent source of tumor DNA for genomic analysis in lieu of fresh or frozen samples.

Various ways of multimodal analysis of solid tumors have been reported. One example successfully combined immunostaining and fluorescent *in situ* hybridization (FISH) to co-visualize protein expression and chromosomal aberrations [16-19]. Zhang et al. [19] reported a study combining estrogen receptor expression and the detection of partial deletion in a tumor suppressor chromosomal region in breast carcinoma cell lines. Ye et al. [17] reported the use of combined multi-color FISH and immmunostaining and its importance in future and clinical cancer research. A combined morphological and cytogenetic approach to detect minimal residual disease in leukemia was reported by Grimwade and Freeman [20]. Similarly, a simultaneous visualization of HER2 protein by IHC and gene copy number variation by *in situ* hybridization has been reported by Nitta et al. [21].

Even though there have been several reports of combining IHC and FISH analysis, no systematic study has been reported evaluating the integrity of DNA obtained from IHC-stained sections. The suitability of using such DNA in PCR-based applications, compared to DNA obtained from unstained sections has not been established. In this study, we evaluated the ability to isolate genomic DNA (gDNA) from tissue sections that have previously been used for IHC. We compared the quality and quantity of gDNA recovered from IHC-stained sections to that obtained from unstained sections. Subsequently, we studied the sensitivity and specificity of detecting oncogenic hotspot mutations using quantitative real-time PCR (qRT-PCR) on gDNA obtained from each section.

Materials and Methods

Tumor specimens

Matched unstained and IHC-stained sections from FFPE tissues derived from 31 patients were obtained from the Genentech human tissue repository for performing this study. From an additional 68 patients, IHC-stained sections were obtained where additional unstained sections were not available. All patients had appropriate IRB (Institutional Review Board) approval and informed consent.

Sample preparation

FFPE tissue sections of 4-5 µm thickness were cut from an archival tissue block and mounted on microscope slides. One section was used for hematoxylin and eosin (H&E) staining and evaluated for histopathological features to confirm diagnosis, tumor content, and was marked to exclude non-tumor tissue in downstream analysis. IHC was performed on tumor tissue sections mounted on glass slides. All IHC steps were carried out on the Ventana Discovery XT automated staining platform (Ventana Medical Systems, Tucson, AZ). Sections were treated with cell conditioning solution, then incubated with specific primary antibody for 1 to 2 hours. Specifically bound primary antibody was detected using the Ultraview detection system (Ventana Medical Systems, Tucson, AZ) and counterstained with Hematoxylin II (Ventana Medical Systems, Tucson, AZ), dehydrated, and coverslipped. Tumors were scored 0 (no signal) to 3 (strong signal) based on staining intensity in ≥50% of tumor cells. Following IHC staining and scoring, stained slides were stored at ambient temperature for 1 to 3 years.

Genomic DNA isolation

IHC-stained sections were immersed in xylene for 1 to 5 days until the coverslips fell off the microscope slides. IHC-stained and unstained sections were treated with a xylene substitute (Envirene, Hardy Diagnostics, Santa Maria, CA) to remove paraffin, followed by two ethanol washes for 2 minutes and 3 minutes, respectively. Sections were air-dried and non-tumor areas removed using a sterile scalpel. The remaining tumor tissue was scraped into a tube containing Proteinase K lysis buffer and gDNA was extracted using the QIAamp DNA FFPE Tissue Kit following manufacturer's instructions (Qiagen, Valencia, CA). The gDNA isolated was quantified using Nanodrop (NanoDrop Products, Wilmington, DE). The quality of gDNA was assessed using multiplex PCR assays as described below.

Determination of DNA quality

DNA quality was assessed using a multiplex-PCR method [22] as well as qRT-PCR of commonly used reference genes. The multiplex PCR assay consisted of five primer sets derived from the NCBI UniSTS database in which 5 amplicons of increasing size, from 135 bp to 295 bp were amplified by PCR. A pre-amplification step was added to reduce the amount of DNA required to perform the assays. Multiplex primer mix, 10 µM, was prepared by combining 10 primers at a final concentration of 1 µM per primer. Each PCR reaction contained 25 µL of JumpStart RedTaq ReadyMix (Sigma-Aldrich, St. Louis, MO), 3 µL of 25 mM $MgCl_2$ (1.5 mM final), 1 µL of primer mix (0.2 µM final) and 5 µL of template DNA (25 to 100 ng) in a final volume of 50 µL. Reactions were assembled at room temperature. PCR reactions were run as follows: 94°C (2 min), then 35 cycles at 94°C (1 min), 60°C (1 min), and 72°C (1 min), followed by a final extension at 72°C (7 min). 5 µL of each PCR product was loaded directly onto a 4% agarose gel for electrophoresis. qRT-PCR was performed using equal amounts of DNA (25 ng) from both IHC-stained and unstained FFPE sections on the ABI 7900 Sequence Detection System (Applied Biosystems, Foster City, CA). TaqMan amplification reactions were set up in a reaction volume of 10 µL using the SYBR® Green PCR Master Mix (Applied Biosystem, Foster City, CA) and 200 nM of each primer for GAPDH, Beta Actin and *LINE1* genes. qRT-PCR was performed in 384-well reaction optical plates in duplicate. Thermal cycling conditions were 95°C (10 min), then 40 cycles at 95°C (15 sec) and 60° C (1 min). Data was analyzed using SDS analysis software (Applied Biosystems, Foster City, CA) to determine cycle threshold (C_T) values.

gDNA pre-amplification for mutation analysis

Twenty ng of gDNA was pre-amplified in 10 µL reactions on a 96-well plate, using a pre-amplification primer cocktail [15] in the presence of 1x TaqMan® PreAmp Master Mix (Applied Biosystems; Foster City, CA). Primer concentrations were maintained at 100 nM during the amplification reaction. Samples were pre-amplified using a Tetrad Thermal Cycler (BioRad; Hercules, CA) using the following protocol: 95°C (10 min), followed by 16 cycles at 95°C (15 sec) and 60°C (2 min). Samples were diluted 10-fold, mixed, centrifuged at 3500 rpm and stored at –20°C. To prevent amplicon contamination, separate workspaces and pipettes were used for pre-amplification reaction setup and for dilutions following pre-amplifications. Pre-amplified samples were diluted 1:10 inside PCR

Citation: Desai R, Patel R, Amler L, Koeppen H, McCaffery I, et al. (2015) A Novel Method for Mutation Analysis Using Genomic DNA Obtained from Immunohistochemistry-Stained Sections. J Mol Biomark Diagn 6: 228. doi:10.4172/2155-9929.1000228

hoods that were UV-irradiated before each use to prevent amplicon contamination.

Mutation analysis

Mutations in *BRAF, NRAS*, and *PIK3CA* were detected using Taqman assays that were developed and validated in-house [23]. Details of primers and probes sequences are described by Patel et al. [15]. 1.25 µL of the pre-amplified, diluted DNA was run in each mutation assay reaction along with TaqMan Master Mix (Applied Biosystems, CA) and 900 nM each of forward and reverse PCR primers were added. 200 nM of two TaqMan MGB probes: one specific to the wild-type allele labeled with VIC, and the other specific to the mutant allele labeled with 6-FAM were added. Reactions were carried out in 384-well plates using an ABI 7900HT Sequence Detection System (Applied Biosystems, CA) in duplicate. The following thermal cycling conditions were used: 50°C (2 min) and 95°C (8 min), followed by 40 cycles at 95°C (10 s) and 61°C (30 s). Mutations in *KRAS* were detected using the Therascreen® KRAS Mutation kit (Qiagen, Velencia, CA) following the manufacturer's instructions using pre-amplified DNA.

C_T values were determined for each qRT-PCR assay using SDS analysis software (Applied Biosystems, Foster City, CA), and mutation calls were made based on the ΔC_T values between wild-type and mutant alleles for both TaqMan and DxS assays. An assay was considered valid when the C_T of wild-type assay was ≤30, and invalid or ' no call' when the C_T was >30. For Therascreen KRAS assays, samples were determined to be mutant if ΔC_T was above the pre-specified cut-off for each assay. For *NRAS, BRAF* and *PIK3CA* mutation detection assays, samples were considered mutant when the ΔC_T values were ≤6 and mutation not detected (MND) when ΔC_T values were >6.

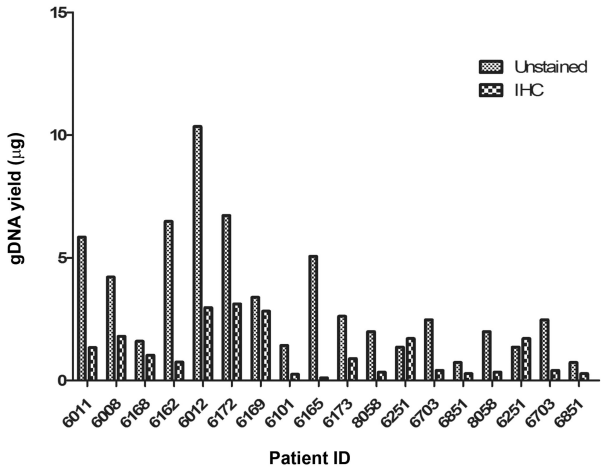

Figure 1: gDNA yield from IHC-stained tissue sections and their unstained counterparts.

Results

The amount of gDNA obtained from IHC-stained sections and their unstained counterparts are summarized in Figure 1. In general, IHC-stained FFPE sections yielded less gDNA compared to unstained sections. The yield of DNA from the IHC-stained samples was up to 48-fold less than their unstained counterparts but in most cases it was still sufficient to carry out mutation analysis.

The quality of DNA obtained from unstained and IHC-stained FFPE sections was assessed to determine whether the quality was adequate for qRT-PCR. Multiplexed PCR analysis followed by gel electrophoresis showed that the quality of DNA obtained from stained and unstained sections was comparable (Figure 2). Despite lower yields, when equal amounts (25 ng) of gDNA from IHC-stained and unstained FFPE sections were amplified by real time PCR, similar C_T values were obtained for target genes GAPDH, Beta Actin, and *LINE1*. These results are summarized in Figure 3 suggesting that DNA integrity is maintained through the IHC-staining and subsequent storage.

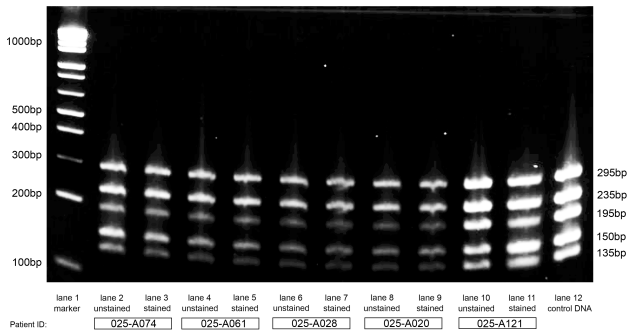

Figure 2: Quality assessment of gDNA isolated from IHC-stained tissue sections and their unstained counterparts by multiplex PCR and gel electrophoresis.

The mutation detection method was validated using patient samples from clinical studies harboring known oncogenic mutations. Thirty-one FFPE samples with known mutations were analyzed and 100% concordance was observed in their mutational status (Table 1). Further, in order to confirm the reproducibility and consistency of data obtained, two independent IHC-stained sections from the same patient were processed separately for 9 samples, gDNA isolated and mutation analysis was performed (Table 2). Finally, we applied this method to perform mutation analysis on 68 additional patient samples where unstained sections were not available, and found that we were able to reliably assess their mutation status (wild-type $C_T \leq 30$, Table 3). The quantity of gDNA obtained was too low for 11 samples (16%) to make a reliable assessment (Wild-type C_T>30).

Citation: Desai R, Patel R, Amler L, Koeppen H, McCaffery I, et al. (2015) A Novel Method for Mutation Analysis Using Genomic DNA Obtained from Immunohistochemistry-Stained Sections. J Mol Biomark Diagn 6: 228. doi:10.4172/2155-9929.1000228

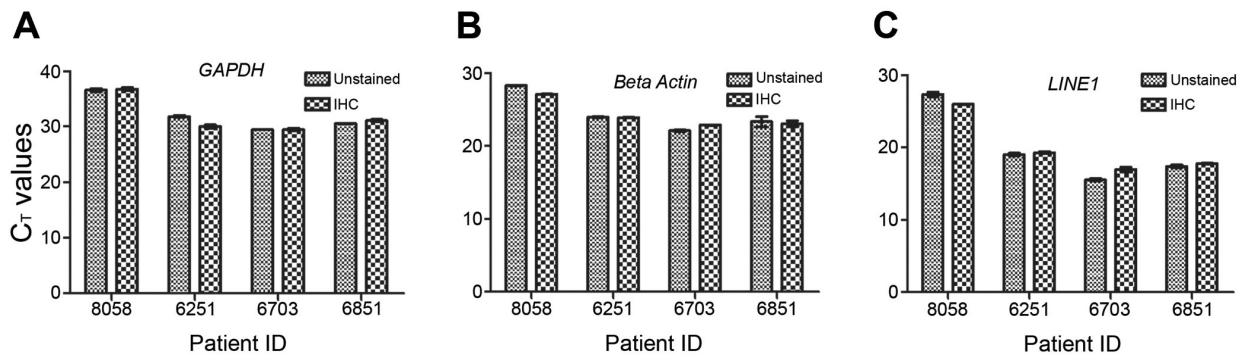

Figure 3: qRT-PCR using 25 ng of DNA from IHC-stained and unstained sections (A) *GAPDH*, (B) *Beta Actin,* and (C) *LINE1.*

			Stained		Unstained	
Patient ID	**Tissues**	**Gene/Mutation**	**Wild-type C_T**	**Mutant C_T**	**Wild-type C_T**	**Mutant C_T**
6012	Colorectal	MND	25.1		26.3	
6165	Colon	MND	25.2		24.8	
6172	Rectum	MND	24.8		24.1	
6173	Colon	MND	24.8		24.2	
1703	Breast	*PIK3CA*, 1047R	26.7	30.3	19.0	23.4
1740	Breast	MND	24.8		21.6	
1743	Breast	*PIK3CA*, E545K	26.7	30.1	18.8	22.6
1786	Breast	MND	25.2		19.9	
2282	Breast	*PIK3CA*, E545K	19.8	21.0	18.6	21.7
2286	Breast	MND	27.5		18.4	
2317	Breast	MND	22.9		18.7	
2485	Breast	MND	18.8		19.0	
2643	Breast	MND	25.6		18.2	
2765	Breast	MND	24.1		19.3	
3064	Breast	MND	27.6		17.6	
3528	Breast	MND	29.2		18.3	
3565	Breast	*PIK3CA*, H1047R	23.3	26.3	18.2	23.3
3582	Breast	MND	24.8		18.9	
3659	Breast	MND	26.1		21.1	
3849	Breast	MND	21.9		18.5	
3920	Breast	MND	28.7		18.8	
025-A074	Colorectal	*Kras*, G13D	28.2	33.2	24.5	26.2
025-A090	Colorectal	*Kras*, G12A	28.0	28.2	24.9	24.0
025-A027	Colorectal	*Kras,* G12A	28.0	29.9	24.8	26.2

Citation: Desai R, Patel R, Amler L, Koeppen H, McCaffery I, et al. (2015) A Novel Method for Mutation Analysis Using Genomic DNA Obtained from Immunohistochemistry-Stained Sections. J Mol Biomark Diagn 6: 228. doi:10.4172/2155-9929.1000228

025-A020	Colorectal	MND	21.5	32.3	21.0	
025-A020	Colorectal	MND	24.2	37.6	23.1	
025-A072	Colorectal	*Kras,* G13D	22.3	26.0	24.1	25.6
025-A061	Colorectal	*Nras,* Q61R	21.3	22.5	19.6	21.0
025-A121	Colorectal	*Nras,* Q61K	25.2	25.7	21.4	22.8
025-A028	Colorectal	*BRAF*, V600E	16.2	19.0	15.7	19.0
025-A028	Colorectal	*BRAF,* V600E	18.1	21.1	16.8	19.6
C_T: cycle threshold; MND: Mutation not detected						

Table 1: Correlation between mutation calls made using unstained and IHC-stained sections. Mutation analysis was done using TaqMan (*BRAF, NRAS*) and Therascreen® *KRAS* and PI3K Mutation kits.

Patient ID	Tissues	Gene/Mutation	Stained		
			Section	Wild-type C_T	Mutant C_T
025-A090	Colorectal	*Kras*, G12A	1	28.0	28.2
		Kras, G12A	2	29.9	30.2
025-A027	Colorectal	*Kras*, G12A	1	28.0	29.9
		Kras, G12A	2	29.8	32.1
025-A020	Colorectal	MND	1	21.5	32.3
		MND	2	23.3	35.9
025-A020	Colorectal	MND	1	24.2	37.6
		MND	2	24.8	35.1
025-A072	Colorectal	*Kras*, G13D	1	22.3	26.0
		Kras, G13D	2	21.9	25.2
025-A061	Colorectal	*Nras,* Q61R	1	21.3	22.5
		Nras, Q61R	2	20.0	21.8
025-A121	Colorectal	*Nras*, Q61K	1	25.2	25.7
		Nras, Q61K	2	24.7	26.6
025-A028	Colorectal	*BRAF*, V600E	1	16.2	19.0
		BRAF, V600E	2	18.4	23.2
025-A028	Colorectal	*BRAF*, V600E	1	18.1	21.1
		BRAF, V600E	2	19.4	22.4
C_T: Cycle Threshold; MND: Mutation not detected					

Table 2: Reproducibility of two consecutive IHC-stained sections. Mutation analysis was done using TaqMan (*BRAF, NRAS*) and Therascreen® KRAS Mutation kits.

Patient ID	Tissues	Gene/Mutation	Section	Stained	
				Wild-type C_T	Mutant C_T
6169	Colorectal	MND		24.6	
4176	Breast	No call		30.1	32.7
4417	Breast	MND		28.3	
4042	Breast	*PIK3CA*, E542K		27.9	32.9
4152	Breast	MND		25.7	
4126	Breast	No call		34.8	
4396	Breast	No call		33.7	
4092	Breast	No call		33.1	
4367	Breast	MND		27.4	
4146	Breast	No call		32.2	
4340	Breast	MND		29.2	
4332	Breast	*PIK3CA*, H1047R		26.5	29.7
4331	Breast	MND		26.9	
4098	Breast	MND		26.3	
4288	Breast	MND		27.3	
4289	Breast	MND		27.4	
6203	Colorectal	*Kras*, G12V		26.2	28.2
6014	Colorectal	*Kras*, G12D		25.7	26.6
4081	Colorectal	*Kras*, G12V		29.0	30.7
4002	Colorectal	MND		24.3	
4091	Colorectal	*Kras*, G12D		25.6	28.5
4088	Colorectal	MND		26.3	
4087	Colorectal	MND		26.0	
2302	Breast	MND		27.1	
3841	Breast	MND		29.7	
2520	Breast	MND		29.3	

2362	Breast	*PIK3CA*, E545K/D	27.6	29.65
3803	Breast	MND	27.3	
2309	Breast	No call	31.0	
3500	Breast	MND	26.5	
2503	Breast	MND	25.3	
3020	Breast	MND	26.0	
3641	Breast	MND	26.6	
2044	Breast	MND	25.4	
4003	Breast	*PIK3CA*, H1047R	29.1	32.51
2363	Breast	No call	30.5	
3069	Breast	No call	30.6	
4005	Breast	MND	27.2	
2342	Breast	MND	27.5	
3700	Breast	MND	25.0	
2314	Breast	No call	30.4	
2529	Breast	MND	26.5	
3022	Breast	MND	29.2	
3940	Breast	MND	25.6	
3703	Breast	*PIK3CA*, E545K/D	24.6	25.7
3701	Breast	MND	28.4	
4041	Breast	*PIK3CA*, E545K/D	24.1	32.4
3704	Breast	No call	31.9	
2367	Breast	MND	25.6	
3560	Breast	*PIK3CA*, E545K/D	29.1	34.3
1961	Breast	MND	25.5	
2480	Breast	MND	25.6	
1620	Breast	MND	26.6	
3605	Breast	MND	28.4	
2985	Breast	MND	22.0	
3655	Breast	MND	25.7	
3653	Breast	MND	24.8	
3942	Breast	MND	23.2	
3052	Breast	MND	21.4	
3658	Breast	MND	26.9	
2661	Breast	MND	22.2	
3567	Breast	MND	26.5	
2767	Breast	No call	30.4	
2160	Breast	MND	25.5	
3853	Breast	MND	25.2	
2946	Breast	MND	22.8	
2145	Breast	MND	21.1	
2947	Breast	MND	24.8	
C_T: Cycle Threshold; MND: Mutation not detected				

Table 3: Unstained sections not available for these samples, mutation analysis was done using IHC stained sections.

Discussion

We have developed a method for isolating gDNA from tissue sections initially used for IHC staining and subsequently stored at ambient temperature for up to 1 to 3 years. The data presented here indicate that the quality of DNA obtained from IHC-stained sections is comparable to those obtained from their unstained counterparts. We analyzed multiple IHC sections from the same tissue sample and were able to demonstrate the reproducibility of the entire process. The quantity of gDNA obtained from these sections may be much lower than unstained sections. This depends on various factors such as the duration of sample exposure to aqueous phase during IHC staining, number of washes performed during IHC staining, and incubation temperatures. In some instances as shown in Figure 1, the DNA obtained from such sections may be too little for making a reliable assessment. However, given sufficient quantity, we demonstrate that the integrity of gDNA is maintained through the process to enable mutation analysis. We also demonstrate that we were able to reliably discriminate between closely-related mutations such as G12A, G12D, and G12V for KRAS. Our results suggest that the gDNA obtained from these FFPE sections may also be suitable for other applications such as sequencing or mass spectrometry.

Thus, we have demonstrated that it is possible to perform IHC followed by genomic analysis using a single 5 μM section of FFPE tissue. Such an approach is extremely valuable in instances where the availability of tissue is limited. We believe that such multimodal analysis approaches will enable diagnostic testing for targeted therapies and personalized healthcare.

Acknowledgement

We thank Carmina Espiritu, Marvin Au, Alexandra Minn for help with acquisition of clinical tumor tissue samples and IHC stained sections, Linda Rangell for immunohistochemistry support, and Jill Spoerke for reviewing the final manuscript.

References

1. Macconaill LE, Garraway LA (2010) Clinical implications of the cancer genome. J Clin Oncol 28: 5219-5228.
2. Tomczak K, Czerwiaska P, Wiznerowicz M (2015) The Cancer Genome Atlas (TCGA): an immeasurable source of knowledge. Contemp Oncol (Pozn) 19: A68-77.
3. Barbieri CE, Tomlins SA (2015) Reprint of: The prostate cancer genome: Perspectives and potential. Urol Oncol 33: 95-102.
4. Korpanty GJ, Graham DM, Vincent MD, Leighl NB (2014) Biomarkers That Currently Affect Clinical Practice in Lung Cancer: EGFR, ALK, MET, ROS-, and KRAS. Front Oncol 4: 204.

5. Zoratto F, Rossi L, Verrico M, Papa A, Basso E, et al. (2014) Focus on genetic and epigenetic events of colorectal cancer pathogenesis: implications for molecular diagnosis. Tumour Biol 35: 6195-6206.
6. Chapman PB, Hauschild A, Robert C, Haanen JB, Ascierto P, et al. (2011) Improved survival with vemurafenib in melanoma with BRAF V600E mutation. N Engl J Med 364: 2507-2516.
7. Ravnan MC, Matalka MS (2012) Vemurafenib in patients with BRAF V600E mutation-positive advanced melanoma. Clin Ther 34: 1474-1486.
8. Ou SH1 (2011) Crizotinib: a novel and first-in-class multitargeted tyrosine kinase inhibitor for the treatment of anaplastic lymphoma kinase rearranged non-small cell lung cancer and beyond. Drug Des Devel Ther 5: 471-485.
9. Scagliotti G, Stahel RA, Rosell R, Thatcher N, Soria JC (2012) ALK translocation and crizotinib in non-small cell lung cancer: an evolving paradigm in oncology drug development. Eur J Cancer 48: 961-973.
10. Cricca M, Bonvicini F, Venturoli S, Ambretti S, Gallinella G, et al. (2004) Efficient treatment of paraffin-embedded cervical tissue for HPV DNA testing by HC-II and PCR assays. J Clin Virol 29: 137-140.
11. Ferrer I, Armstrong J, Capellari S, Parchi P, Arzberger T, et al. (2007) Effects of formalin fixation, paraffin embedding, and time of storage on DNA preservation in brain tissue: a BrainNet Europe study. Brain Pathol 17: 297-303.
12. Talaulikar D, Gray JX, Shadbolt B, McNiven M, Dahlstrom JE (2008) A comparative study of the quality of DNA obtained from fresh frozen and formalin-fixed decalcified paraffin-embedded bone marrow trephine biopsy specimens using two different methods. J Clin Pathol 61: 119-123.
13. Jacobson TA, Lundahl J, Mellstedt H, Moshfegh A (2011) Gene expression analysis using long-term preserved formalin-fixed and paraffin-embedded tissue of non-small cell lung cancer. Int J Oncol 38: 1075-1081.
14. Pikor LA, Enfield KS, Cameron H, Lam WL (2011) DNA extraction from paraffin embedded material for genetic and epigenetic analyses. J Vis Exp.
15. Patel R, Tsan A, Tam R, Desai R, Spoerke J, et al. (2012) Mutation scanning using MUT-MAP, a high-throughput, microfluidic chip-based, multi-analyte panel. PLoS One 7: e51153.
16. Teerenhovi L, Knuutila S, Ekblom M, Rossi L, Borgström GH, et al. (1984) A method for simultaneous study of the karyotype, morphology, and immunologic phenotype of mitotic cells in hematologic malignancies. Blood 64: 1116-1122.
17. Ye CJ, Stevens JB, Liu G, Ye KJ, Yang F, et al. (2006) Combined multicolor-FISH and immunostaining. Cytogenet Genome Res 114: 227-234.
18. Bedell V, Forman SJ, Gaal K, Pullarkat V, Weiss LM, et al. (2007) Successful application of a direct detection slide-based sequential phenotype/genotype assay using archived bone marrow smears and paraffin embedded tissue sections. J Mol Diagn 9: 589-597.
19. Zhang Y, Siebert R, Matthiesen P, Harder S, Theile M, et al. (2000) Feasibility of simultaneous fluorescence immunophenotyping and fluorescence in situ hybridization study for the detection of estrogen receptor expression and deletions of the estrogen receptor gene in breast carcinoma cell lines. Virchows Arch 436: 271-275.
20. David Grimwade D, Freeman SD (2014) Defining minimal residual disease in acute myeloid leukemia: which platforms are ready for "prime time"? Blood 124: 3345-3355.
21. Nitta H, Kelly BD, Padilla M, Wick N, Brunhoeber P, et al. (2012) A gene-protein assay for human epidermal growth factor receptor (HER2): brightfield tricolor visualization of HER2 protein, the HER2 gene, and chromosome 17 centromere (CEN17) in formalin-fixed, paraffin-embedded breast cancer tissue sections. Diagn Pathol 7: 60.
22. van Beers EH, Joosse SA, Ligtenberg MJ, Fles R, Hogervorst FB, et al. (2006) A multiplex PCR predictor for aCGH success of FFPE samples. Br J Cancer 94: 333-337.
23. Spoerke JM, O'Brien C, Huw L, Koeppen H, Fridlyand J, et al. (2012) Phosphoinositide 3-kinase (PI3K) pathway alterations are associated with histologic subtypes and are predictive of sensitivity to PI3K inhibitors in lung cancer preclinical models. Clin Cancer Res 18: 6771-6783.